AD-A068 817 STATE UNIV OF NEW YORK AT BINGHAMTON F/G 9/2
TEXTURE-TONE FEATURE EXTRACTION AND ANALYSIS. PHASE II.(U)
MAR 79 S HSU, E KLIMKO F30602-76-C-0211
UNCLASSIFIED RADC-TR-79-37 NL

1 OF 1
AD
A068817

END
DATE
FILMED
6 --79
DDC

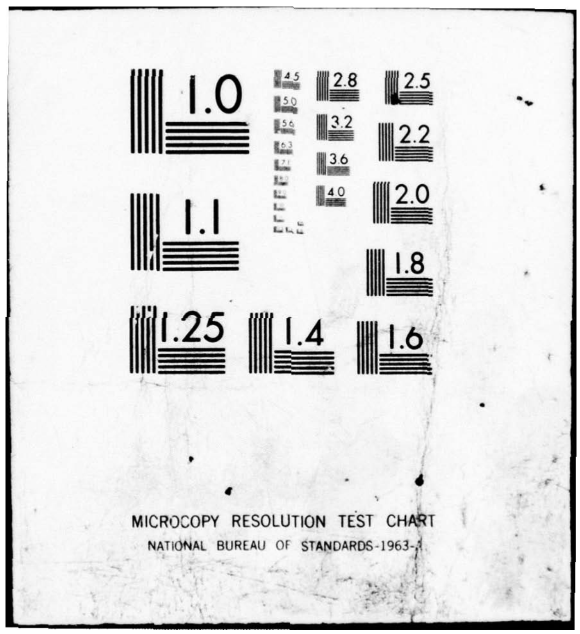
1.0
1.1
1.25
1.4
1.6
1.8
2.0
2.2
2.5
2.8
3.2
3.6
4.0
MICROCOPY RESOLUTION TEST CHART
NATIONAL BUREAU OF STANDARDS-1963-A

RADC-TR-79-37
Final Technical Report
March 1979

TEXTURE-TONE FEATURE EXTRACTION AND ANALYSIS PHASE II

State University of New York at Binghamton

Dr. Shin-yi Hsu
Dr. Eugene Klimko

ROME AIR DEVELOPMENT CENTER
Air Force Systems Command
Griffiss Air Force Base, New York 13441

This report has been reviewed by the RADC Information Office (OI) and is releasable to the National Technical Information Service (NTIS). At NTIS it will be releasable to the general public, including foreign nations.

RADC-TR-79-37 has been reviewed and is approved for publication.

APPROVED:

DONALD A. BUSH
Project Engineer

APPROVED:

HOWARD DAVIS
Technical Director
Intelligence & Reconnaissance Division

FOR THE COMMANDER:

JOHN P. HUSS
Acting Chief, Plans Office

If your address has changed or if you wish to be removed from the RADC mailing list, or if the addressee is no longer employed by your organization, please notify RADC (IRRE), Griffiss AFB NY 13441. This will assist us in maintaining a current mailing list.

Do not return this copy. Retain or destroy.

15 May 79

CONVERSATION RECORD	1. DATE 5/14/79	2. TIME
3. TYPE OF CONVERSATION ☐ TELEPHONE (*Incoming*) ☐ TELEPHONE (*Outgoing*) ☐ OFFICE VISIT		
4. SUBJECT OF CONVERSATION		
5. CALL/VISIT MADE BY (*Name of person*) Ms. Joyce Watkins	5a. OFFICE/FIRM/COMPANY, ETC. RADC	5b. PHONE NO. AND/OR EXT. 8/587-4475
6. CALL/VISIT MADE TO (*Name of person*)	6a. OFFICE/FIRM/COMPANY, ETC.	6b. PHONE NO. AND/OR EXT.

7. SUMMARY OF CONVERSATION, AND IF APPLICABLE, STATEMENT AS TO SUBSEQUENT ACTION TAKEN OR TO BE TAKEN

RADC-TR-79-37 (U) correct

DD Form 1473 reads -78-37

Title: Texture tone feature extraction + analysis phase II.

Apr. 79

(*IF ADDITIONAL SPACE IS NEEDED, CONTINUE ON REVERSE SIDE*)

8. PRINTED NAME AND TITLE OF PERSON MAKING/RECEIVING CALL/VISIT	8a. SIGNATURE

DLA FORM NOV 73 1349 — REPLACES ALL SIMILAR PURPOSE FORMS USED IN DLA, WHICH MAY BE USED UNTIL EXHAUSTED

UNCLASSIFIED

SECURITY CLASSIFICATION OF THIS PAGE (When Data Entered)

REPORT DOCUMENTATION PAGE

READ INSTRUCTIONS BEFORE COMPLETING FORM

1. REPORT NUMBER: RADC-TR-79-37	2. GOVT ACCESSION NO.
3. RECIPIENT'S CATALOG NUMBER	
4. TITLE (and Subtitle): TEXTURE-TONE FEATURE EXTRACTION AND ANALYSIS. PHASE II.	5. TYPE OF REPORT & PERIOD COVERED: Final Technical Rep[redacted]rt. 1 June 77 - 30 Sep[redacted] 78.
	6. PERFORMING ORG. REPORT NUMBER: N/A
7. AUTHOR(s): Dr. Shin-yi Hsu, Dr. Eugene Klimko	8. CONTRACT OR GRANT NUMBER(s): F30602-76-C-0211
9. PERFORMING ORGANIZATION NAME AND ADDRESS: State University of New York at Binghamton, Binghamton NY 13901	10. PROGRAM ELEMENT, PROJECT, TASK AREA & WORK UNIT NUMBERS: 62702F, 62441067
11. CONTROLLING OFFICE NAME AND ADDRESS: Rome Air Development Center (IRRE), Griffiss AFB NY 13441	12. REPORT DATE: Mar[redacted]79
	13. NUMBER OF PAGES: 62
14. MONITORING AGENCY NAME & ADDRESS (if different from Controlling Office): Same	15. SECURITY CLASS. (of this report): UNCLASSIFIED
	15a. DECLASSIFICATION DOWNGRADING SCHEDULE: N/A

16. DISTRIBUTION STATEMENT (of this Report)

Approved for public release; distribution unlimited

17. DISTRIBUTION STATEMENT (of the abstract entered in Block 20, if different from Report)

Same

18. SUPPLEMENTARY NOTES

RADC Project Engineer:

Donald A. Bush (IRRE)

19. KEY WORDS (Continue on reverse side if necessary and identify by block number)

Texture Analysis	LANDSAT images/texture characteristics
Texture feature extraction	Estimation of stable parameter
Normal Mahalanobis classifier	Digitized B/W Photography
Stable Mahalanobis classifier	Hit-rate analysis
Stable distribution	Automatic selection of training sets

20. ABSTRACT (Continue on reverse side if necessary and identify by block number)

Since more than 50 percent of the 17 texture feature variables developed in our Phase I effort are not normally distributed, a non-linear classified based on stable distribution model was developed to accommodate the skewness characteristics of the texture data and thus improve the hit-rate of the decision maps of the text sets. With this classifier the needed texture feature variables have been reduced to 3 from the original 17, resulting in a drastic improvement in the processing rate, i.e., a factor of 6 (times faster) has been achieved (from 90 minutes CPU to 15 minutes CPU with IBM 370-158 system). Currently the processing

DD FORM 1 JAN 73 1473

UNCLASSIFIED

SECURITY CLASSIFICATION OF THIS PAGE (When Data Entered)

333 220

rate for (256 x 256) pixels with the ITEL AS-6 system is less than 4 minutes with FORTRAN programming language.

The new classifier was able to improve the hit-rate by about 5 percentage points with an average hit-rate of 90 percent or higher. In addition, the amount of rejects has also been reduced.

With a manual method of the selection of training sets, the amount of rejects remains high even though a better classifier was utilized in the analysis. To solve this problem, an automatic selection of training sets technique was developed with the intention that the rejects be included in the clusterings derived from randomly selected pixels from the test sets. With this method, the amount of rejects has been reduced to 3 percent or less from 20 to 30 percent.

In this effort, LANDSAT data were also analyzed to determine their value for feature extraction. With experiments from three subscenes from the Pheonix, AZ frame, it was proved that there exists texture information in the LANDSAT MSS data for feature extraction. Automatic selection of training sets technique is particularly appropriate for the analysis of LANDSAT data since the ground truth information on LANDSAT images is generally difficult to obtain.

PREFACE

This report was prepared by Professor Shin-yi Hsu of the State University of New York, Binghamton, New York in partial fulfillment of Contract 30602-7-C-0211 (supplement), for the Rome Air Development Center, Griffiss Air Force Base, New York. Following the Phase I effort of this contract, the work incorporated in this task consisted of development of a 3-variable feature extractor, analysis of digitized black and white aerial photography and LANDSAT data, and automatic selection of training sets data with imagery texture features. The project was carried out using both the DICIFER Image Processing System of the RADC Image Processing Facility, and the SUNY-Binghamton Image Data Processing Systems.

The work described in this report was performed by Dr. Shin-yi Hsu, Principal Investigator, Dr. Eugene Klimko, Co-investigator, Jane Huang, Research Associate and Timothy Masters, Advanced Graduate Assistant.

This study was performed during the period June 1, 1977 through September 30, 1978. Mr. Don Bush was the RADC Project Monitor.

TABLE OF CONTENTS

Table of Contents (continued)

LIST OF TABLES

EVALUATION

This report represents an approach using three measurements (mean, 1st neighbor contrast and 2nd neighbor contrast) as well as automatic training set selection. The results were a reduction in processing time from 90 minutes to 18 minutes of processing time. These techniques will eventually be tested in the Automatic Feature Extraction System at RADC.

Donald A. Bush

DONALD A. BUSH
Project Engineer

SECTION I

INTRODUCTION AND SUMMARY

As pointed out by Mr. Donald Bush, RADC project engineer, in the "Evaluation" section of the Phase-I report of this contract, our effort represents "a fine tuning of feature extraction and image classification that will be used in applications to the Automatic Feature Extraction System (AFES) being developed at RADC." It is therefore necessary here to mention briefly the intent of AFES. This will serve as an introduction to this report.

From the document, Statement of Work for Automatic Feature Extraction System (RADC, 1976), it is understandable that the manual operation for the Digital Radar Landmass Simulation (DRLMS) is very time-consuming because this manual system can process only 2 nautical miles of image information per hour. To solve this mass data processing problem, the AFES was intended to process 25 square nautical miles per working hour using images at a nominal scale of 1:100,000. The real challenge to AFES is that the system must produce a Feature Analysis Data Table (FADT) which includes such detailed information as percentage roof cover, percentage foliage, percentage stone, brick and/or concrete, percentage metal surface, and the size of the object, and so on.

From the above discussions, it can be concluded that AFES needs an image processing system which is capable of classifying features based on pixels instead of a group of pixels (or scenes) at an extremely fast data processing rate. Intended to assist the development of such a high performance system (AFES), we have developed a 3-variable feature extractor from the original 17-variable system documented in the Phase-I effort (RADC-TR-77-279, Final Technical Report, August, 1977). The net effect has been a drastic reduction in image processing time: from 90 minutes by using 17 features to 15-18 minutes of CPU time with three features regarding processing of (256 x 256) pixels with the IBM 370-158 system using FORTRAN language. In other words, a factor of six (times faster) has been obtained by using a feature extractor containing these three effective texture variables--mean brightness, 1st neighbor contrast, and 2nd neighbor contrast--derived from a (3 x 3) moving grid, which is called Model 1 in the Phase-I report. The processing time has been recently reduced further to about three minutes with the ITEL AS-6 system instead of the IBM 370-158 system.

From an experiment using eight frames of digitized black and white aerial photography and three sub-frames of LANDSAT data, we are able to conclude that the use of fewer variables in the feature extractor can be compensated by (1) the use of a more powerful classifier as compared to the one based on the Gaussian (normal) distribution, and (2) the selection of training sets whose texture variables are fairly normally distributed.

To this end, we have developed a Mahalanobis classifier based on the stable distribution model because, as compared to the normal distribution model, it is capable of incorporating the skewness and tail heaviness parameters of the data in the classifier. To eliminate the non-normal characteristics of the training sets, we have developed an automated selection procedure to replace the manual method which employs a cursor/joystick in conjunction with an image displaying system. In the context of sampling theory, an automated selection of training sets employs a systematic random sampling method, whereas the manual method utilizes a cluster sampling procedure.

The results indicate that the use of these two complementary methods--the stable Mahalanobis classifier and/or automatic selection of training sets--is able to improve the average hit-rate by more than five percentage points in the generation of decision maps as compared to the procedure utilizing the normal Mahalanobis classifier with manually selected training sets.

The main body of this report will include an update of the literature on texture analysis, summary of the Phase-I report, the stable Mahalanobis classifier, automatic selection of training sets, and analysis of the sampled image data (frames).

Finally, the principal investigator would like to express his gratitude to Mr. Donald Bush for his ideas on automated processing of image data and supply of the LANDSAT tapes.

SECTION 2

SUMMARY OF THE PHASE-I EFFORT AND REMAINING QUESTIONS

2.1 ORIGINATION OF THE PHASE-I EFFORT

During 1975 and 1976, using the DICIFER System, RADC conducted a study on automatic terrain classification with digitized black and white photography yielding a correct classification rate of 80 percent. Since the texture feature extractor of the DICIFER system utilized only six variables (mean, standard deviation, range, median, high and low), it was hypothesized that a higher hit-rate could be obtained by using a more powerful feature extractor in the analysis.

To this end, the Phase-I effort of this project was centered around the development of a texture feature extractor using variables derived from a (3 x 3) moving grid, and testing of this texture measure using the same data set for the 1975-76 study.

2.2 RESULTS OF THE PHASE-I EFFORT

2.2.1 A New Texture Measurement

Intended to classify individual pixels, a texture measure with the following 17 variables was developed: (1) through (4) are the four central moments, (5) is the absolute deviation, (6) is the contrast of the center point from its neighbors, (7) is the mean brightness of the center point relative to its background, (8) is the contrast between adjacent neighbors, (9) is the sum of squared value of (8), (10) is the contrast between the second neighbor, (11) is the sum of the squared value of (10), and (12) through (17) are the mean area above and below three datum planes (50, 100, 150). The code name and computational formula of these variables are given in Table 2-1.

Using a stepwise discriminant analysis procedure, it was determined that, excepting skewness and kurtosis, these feature variables were significant in contributing to the power of discrimination among terrain types including soil, vegetation, cultivated fields, metal, water, and composition (mixture of a number of classes). Thus, all of these variables were utilized in the analysis in conjunction with the Mahalanobis classifier based on the normal distribution model.

TABLE 2-1. The Texture Variables From (3 x 3) Grid Design

	Code	Description or Computational Formula	
1.	MEAN	average	
2.	STD	standard deviation	the four
3.	SKEW	skewness	central moments
4.	KURT	kurtosis	
5.	MDEVN	$\Sigma \lvert x_i - \bar{x} \rvert / n$, where x = tone value of individual pixels; $\bar{x}$ = mean	
6.	MPTCON	$\Sigma \lvert x_i - x_c \rvert / n$, where x_c = tone value of the center point	
7.	MPTREL	$\Sigma (x_c - x_i)/n$	
8.	MINCON	$\Sigma \lvert x_i - x_j \rvert / n$, i and j are adjacent pixels	
9.	MINSQR	$\Sigma (x_i - x_j)^2 / n$	
10.	M2NCON	$\Sigma \lvert x_i - x_k \rvert / n$, x_c and x_k are second nearest neighbors	
11.	M2NSQR	$\Sigma (x_i - x_k)^2 / n$	
12.	MADAT1	numerical calculation of mean area above datum 1 (50)	
13.	MADAT2	mean area above datum 2 (100)	
14.	MADAT3	mean area above datum 1 (50)	
15.	MBDAT1	mean area below datum 1 (50)	
16.	MBDAT2	mean area below datum 2 (100)	
17.	MBDAT3	mean area below datum 3 (150)	

2.2.2 The Mahalanobis Classifier

In our previous report, the Mahalanobis classifier is defined as:

$$D_i^2 = (Y - U_i)^T (Q_i)^- (Y - U_i) \quad (1)$$

where Y is the unknown pixel

U_i is centroid of each training set

Q_i is dispersion matrix of each training set

T stands for transpose of a matrix

- stands for the generalized inverse of a matrix.

Then the classification rule becomes: assign Y to population i if $D_i^2 = \min [D_1^2,\ldots,D_k^2]$. (See also Morrison, 1976 and Glick, 1977.)

Compared to the conventional classifiers described by Nalepka (1970), this Mahalanobis classifier has two unique features: (a) it utilizes separate dispersion matrices for each training set as opposed to a pooled dispersion matrix, in equation (1), and (b) it employs a generalized inverse procedure instead of the conventional matrix inversion method to invert individual dispersion matrices.

The use of the generalized inverse here is to accommodate the singular matrices inherited in the 17 texture variables of individual training sets. Using a computation formula singularity of dispersion matrices can be assessed by determining the rank of matrix by discarding the eigenvalues which is less than a threshold measure defined as follows:

$$\frac{\text{given eigenvalue}}{\text{largest eigenvalue}} < 10^{-4} \quad (2)$$

Table 2-2 shows singularity of the 17 texture variables.

One can realize, from Table 2-2, that the pattern of rank deficiency varies with each training set; therefore, there is no "common" texture variables that can be discarded to avoid singularity with respect to all of the training sets. The use of the generalized inverse can easily take care of this problem.

The computational formula for obtaining the generalized inverse is given by Searle (1971), whereas the theory and applications of the generalized inverse of matrices were discussed by Rao and Mitra (1971).

TABLE 2-2. Singularity in Texture Variables

	Training Sets	Total Texture Variables	Rank of the Data Set	Rank Deficiency
1.	Cultivated Field 1	17	12	5
2.	Cultivated Field 2	17	12	5
3.	Soil 1	17	13	4
4.	Soil 2	17	13	4
5.	Vegetation 1	17	11	6
6.	Vegetation 2	17	13	4

Once singularity of matrices is solved, we can employ individual dispersion matrices for each training set in the classifier. It has been determined that an improvement of about eight percentage points can be obtained by using unpooled data in the training sets alone. Table 2-3 indicates such a result.

TABLE 2-3. A Comparison in the Hit-Rate

A. Confusion matrix with pooled dispersion matrix.

	Pavement	Vegetation	C. Field 1	Soil	Composition	C. Field 2
Pavement	29	0	0	2	15	0
Vegetation	0	111	0	0	0	64
C. Field 1	0	41	293	0	0	1
Soil	5	0	5	89	1	0
Composition	22	0	11	0	42	0
C. Field 2	1	52	5	0	0	170

Correct Classification Rate: 76.5%

B. Confusion matrix with unpooled dispersion matrices.

	Pavement	Vegetation	C. Field 1	Soil	Composition	C. Field 2
Pavement	43	0	0	1	2	0
Vegetation	0	81	8	0	0	86
C. Field 1	6	5	289	0	35	6
Soil	0	0	1	95	4	0
Composition	1	0	2	0	72	0
C. Field 2	0	0	0	0	0	228

Correct Classification Rate: 84.25%

2.2.3 Experimental Results

Using the same data sets for the 1975-76 RADC study (RADC-TR-76-196, Final Report by PAR), we analyzed eight scenes of the RADC's Northeast Test Area (four low altitude and four high altitude U-2 photographs). After digitization the ground resolution of the low altitude and high altitude images are approximately 8.75 feet, and 56.75 feet, respectively.

Using the 17-variable texture extractor in conjunction with the Mahalanobis classifier, we have obtained an average hit-rate of 85-90 percentage, a significant improvement over the original 1975-76 RADC experiment. Table 2-4 indicates the results. We have also assessed the error probability of Table 2-4 is insignificant since the size of the training sets was very large (see Table 2-5). This argument is based on Foley's criterion: for a valid analysis, the minimum size of the training set is three times as large as the number of variables in the discriminent functions (Foley, 1971).

TABLE 2-4. Hit-Rate Analysis of the Test Sets Data

Classes	Vegetation	C. Field	Metal	Soil	Pavement	Water	Composition
Low Altitude							
Frame 1	88.4%	98.46%	90%	53.13%	92.28%	-	-
Frame 2	89.81%	82.59%	-	87.13%	-	-	-
Frame 3	-	-	80.50%	45.90%	85.24%	-	87.4%
Frame 4	90%	85.5%	95.0%	86%	-	-	-
High Altitude							
Frame 5	88.51%		-	85.53%	72%	-	75%
Frame 6	99%	95%	-	98%	-	-	95%
Frame 7	60%	84%	-	83.7%	70%	-	85.1%

TABLE 2-5. The Sizes of the Test Sets, Design Sets and Rejects

	Test Set	Design Set	Rejects*
Frame 1	(252 x 252) = 63,504	2047	0
Frame 2	(252 x 252)	1345	0
Frame 3	(252 x 252)	1445	0
Frame 4	(252 x 252)	1127	0
Frame 5	(252 x 252)	584	0
Frame 6	(252 x 252)	612	0
Frame 7	(252 x 252)	1664	0

*Rejects are those pixels dissimilar to the training sets.

2.3 THE OBJECTIVES OF THE PHASE II EFFORT

At the end of our Phase I effort, we determined that there were several image processing methods that could be utilized to improve the classifier and data processing rate because we identified from our experiments the following specific problems:

(1) Approximately 50 percent of our texture variables are not normally distributed,

(2) The correct classification rate in the decision map is highly dependent on the characteristics of the training sets, and

(3) The data processing rate is low since it took about 90 minutes of CPU time to generate a decision map consisting of (256 x 256) pixels using IBM 370-158 system with FORTRAN language.

Therefore, to solve these problems, the Phase II effort was designed to achieve the following objectives:

(1) To develop a classifier based on the stable distribution model instead of the Gaussian distribution so that the skewness and kurtosis characteristics of the image texture data can be taken into consideration in the analysis,

(2) To design a sampling/analysis method by which the training sets can be selected automatically so as to eliminate "misrepresentation" of the test set by the design sets, and

(3) to select from the 17 texture variables a few, but most effective measures for the feature extractor so that the data processing time can be reduced.

These experiments utilized the same data sets for the Phase I work, plus a scene of LANDSAT (tape).

SECTION 3

THE STABLE MAHALANOBIS CLASSIFIER

3.1 CHARACTERISTICS OF THE IMAGERY TEXTURE DATA

It has been well documented that spectral response data, in most cases, are not normally distributed (Crane, Malina and Richardson, 1972). Therefore, the conventional pattern recognition methods based on the Gaussian distribution model are inappropriate because their normality assumptions are violated by the data, and thus induce a substantial error in the final decision map. To solve this problem as well as to improve the feature extractor, a texture measure with 17 feature variables (Section 2) was developed; it was assumed that the normality problem could be alleviated by using the texture data instead of the multi-spectral (tone) data.

To reveal the distributional characteristics of image data, one can use both graphic displays via histograms and mathematical methods to assess the skewness parameters of the data. Figure 3-1 shows a series of histograms from GALA training sets. For analytical purposes, we have employed two parameters of the stable distribution model to assess the data's departure from a normal distribution; namely, α as the stable index and β as the symmetry parameter. Since for a normal distribution, $\alpha = 2$, and $\beta = 0$, a significant departure from these two indices will indicate that the data is not normal. We have tested eight scenes and determined that approximately 50 percent of the 17 variables are not normally distributed as indicated in Table 2-6 using UPHA as an example.

Therefore, it was hypothesized that a classifier based on the stable distribution instead of the normal distribution would perform better since it can accommodate the skewness characteristics of the image data.

3.2 THE STABLE DISTRIBUTION MODEL AS A CLASSIFIER

3.2.1 Introduction

In our Phase-I report, we pointed out the significance of using stable distributions to model the image data based upon a well known principle: the better a model can describe the characteristics of the data, the higher the hit-rate the model can produce. Since the image texture data are highly skewed specifically the training sets are obtained by means of a manual selection method (Table 3-1). We expect that the stable distribution model can produce a better result as compared to the normal distribution model.

Stable distributions are best described by their characteristic functions $\phi(t)$ or its logarithm which in the univariate case is given by

$$\log_e \phi(t) = \log_e \int_{-s}^{s} e^{itx}\, d\, f\,(x)$$

$$= itd - r\,|t|^{\alpha}\left[1 + i\beta \frac{t}{|t|}\, w\,(t, \alpha)\right]$$

where $w\,(t, \alpha) = \tan\,(\pi\alpha/2)$, if $\alpha \neq 1$

$$= \frac{2}{\pi}\, \log\, |t|\ , \text{ if } \alpha = 1 \qquad (3)$$

and δ is a location parameter (comparable to mean), $\gamma \geq 0$ is a scale parameter (comparable to variance), α is the characteristic and β is the symmetry parameter. If $\beta = 0$, the distribution is symmetric. If $\alpha = 2$, then

$$\log\, \phi\,(t) = it\,\delta - rt^2 \qquad (4)$$

which is the characteristic function of a univariate normal distribution with mean δ and variance $\gamma/2$. If $\alpha = 1$ the distribution is cauchy. For all other values of α, the density exists but a closed formula for it is not known. Various power series expansion for the density exist, however (DuMouchel, 1971, Feller, 1966).

3.2.2 Proposed Estimation Method of Stable Parameters

To employ the stable distribution model as a classifier, the four parameter of the distribution (δ, γ, α and β) of the training sets must be estimated first so the distributional characteristic of the data can be described by the model.

The literature on the estimation of stable parameters can be obtained from Fama and Roll (1968, 1971), DuMouchel (1971), Press (1972) and Paulson, Holcomb and Leitch (1975). We have investigated these methods and determined that (1) Fama and Roll's procedure was not precise enough for our purposes, Press' was not usefull, While Paulson, Holcomb and Leith's approach utilized the sample characteristic function, DuMouchel's attacked the problem with maximum likelihood estimation.

Since the number of replications used in Paulson et al is very small, the validity of their procedure cannot be obtained. We also discovered that two drawbacks existed in DuMouchel's method: (1) since the data is censored into discrete classes, some information loss will most likely take place, and (2) computationally, this method is very slow.

Before the stable parameter can be estimated, methods for explicitly evaluating stable densities and distribution functions must be worked out. For this, our approach utilized computation of the Fourier transform of the characteristic function:

$$S(x) = \frac{1}{2} \int_{-s}^{s} \exp(-i x t)\, \phi(t)\, dt \qquad (5)$$

where $\phi(t)$ is the characteristic function of s (x).

DuMouchel (1971) devised a rapid and accurate procedure for the evaluation of this integral using fast Fourier transform. Masters (1977) made some manipulation of the definition of this integral for computational purposes. It was then used to generate a table for future interpolation purposes.

For this project, two estimation methods were developed. Whereas the first approach utilized a maximum likelihood procedure, the second employed two ratios obtained from a series of percentiles (such as 0.05, 0.25, 0.50, 0.75, and 0.95) to characterize the distribution (i.e., departure from normal and skewness) of the data. We employed the second method because (1) it is computationally faster than the maximum likelihood procedure, and (2) it produced approximately the same or better hit-rate in the confusion matrix with the training set data. This is called the fast estimation method in our image processing system.

3.3 THE STABLE DISTRIBUTION MODEL AS A CLASSIFIER

To employ the stable distribution as a classifier, we have developed two methods, first, we developed the stable classifier by using the original stable density function. For this, the mathematical form of the multivariate stable distributions has to be developed first. The classifier can then be designed according to the standard discriminant analysis described by Rao (1973, p. 574). Here it is assumed that the spectral/texture data of the objects have density functions $P_1(x)$,---,$P_k(x)$, where $P_i(x)$ is the density function of objects in the ith class. To classify an unknown object whose spectral response is given as x is to compute the numerical value of P_i (x) for each i = 1, 2, ---, k, and place the object into class i, for which $P_{i_o}(x)$ is the largest. In this study, although we have developed multivariate stable density function, we decided not to program the method for image data classification because the computation process is extremely slow, specifically in view of the fact that it already took 90 minutes of CPU time to process (256 x 256) pixels using 17 texture variables in the Mahalanobis classifier (normal distribution) with the IBM 370-158 system.

The alternative is to use the framework of the (normal) Mahalanobis classifier for the stable distribution. The idea here is to improve the Mahalanobis classifier by using four stable parameters (δ , γ , α and β) instead of two (mean and standard deviation) in the classifier. To do so, we need to develop a method by which the stable distribution (cumulative density) of a given training set can be "projected" into a perfect normal distribution. In reality, this is a non-linear transformation of a stable distribution to a normal distribution.

Let us explain this transformation idea from Figure 3-1.

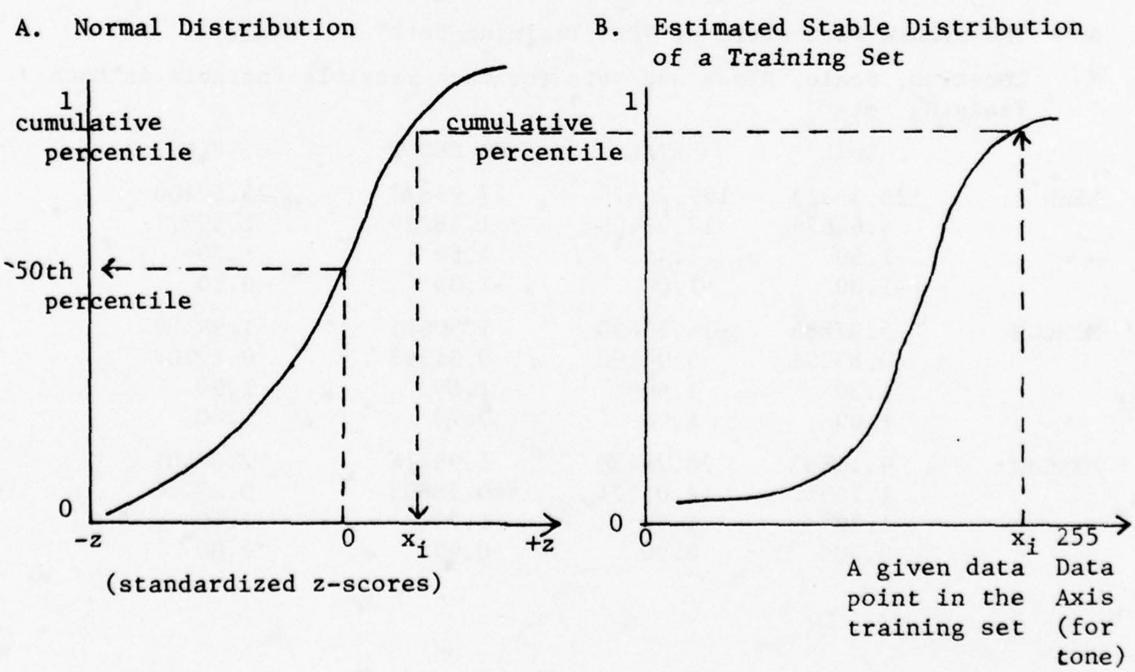

In Figure 3-1(A), we have a normal distribution curve constructed according to the cumulative percentile (y-axis) against the standardized z-scores (with mean 0, variance 1). In Figure 3-1(B), we have an estimated stable distribution for a given training set with y-axis as cumulative percentile, x-axis the raw data. Note that the curve in B is more skewed than that in A. Suppose that there is a pixel x_i distributed on the x-axis. Then its percentile position on the y-axis can be obtained from the estimated stable distribution (curve), say, it is at the 80th percentile. Its normal equivalence after transformation will be the z-score (y-axis) at the 80th percentile point (x_i') in Figure 3-1A.

Once this transformation is performed, the Mahalanobis classifier is applicable to the stable distribution model. In the analysis, normal transformation has to be performed on all of the training sets, and all of the texture feature variables. Table 3-1 is an example of the transformation process using the VPLA frame.

TABLE 3-1. Estimated Stable Parameters and Their Normal Transformations Using the VPLA Frame

A. The Stable Parameters of VPLA Training Sets

Location, Scale, Alpha and Beta for Each Possible Variable in Each Training Set

	SOIL	METAL	C. FLD 1	C. FLD 2
MEAN	125.55615	197.20479	27.99875	25.57103
	4.64679	17.31409	1.58239	1.59771
	1.50	1.40	1.50	1.70
	-1.00	-1.00	-1.00	-0.90
M1NCON	5.37888	14.39490	1.50673	1.94587
	0.83295	5.94790	0.31742	0.21107
	1.30	1.60	1.80	1.90
	1.00	1.00	0.70	0.80
M2NCON	9.16833	28.25470	1.98716	2.32401
	1.76352	12.01571	0.38803	0.27750
	1.30	1.50	1.70	1.80
	0.90	0.90	0.90	1.00

Table 3-1 (continued)

	C. FLD 3	VEGATATN	PAVEMENT	SPORTS
MEAN	14.11572	97.31676	152.86922	58.22362
	1.01325	1.82666	17.62323	9.72661
	1.60	1.01	1.80	1.40
	1.00	0.80	-0.90	1.00
M1NCON	1.88918	14.42804	8.50840	3.68116
	0.25066	0.28722	5.12097	0.55689
	1.90	1.01	1.90	1.20
	0.60	0.70	1.00	1.00
M2NCON	2.05636	31.59818	18.20215	6.35123
	0.36938	0.46485	9.32217	1.22841
	1.90	1.01	1.60	1.20
	0.80	1.00	0.90	1.00

B. Normal Transformation of the Stable Distribution

(1) Means and covariance matrix of normalized variables for training set: SOIL

MEAN	0.000792
M1NCON	0.090528
M2NCON	0.080044

	MEAN	M1NCON	M2NCON
MEAN	0.91787	-0.01419	-0.08212
M1NCON	-0.01419	0.58311	0.55855
M2NCON	-0.08212	0.55855	0.60263

(2) Means and covariance matrix of normalized variables for training set: METAL

MEAN	-0.079429
M1NCON	0.040246
M2NCON	0.062559

	MEAN	M1NCON	M2NCON
MEAN	0.59202	-0.57704	-0.56807
M1NCON	-0.57704	0.61875	0.60052
M2NCON	-0.56807	0.60052	0.58998

(3) Means and covariance matrix of normalized variables for training set: C. FLD 1

MEAN	-0.034767
M1NCON	0.065774
M2NCON	0.061022

	MEAN	M1NCON	M2NCON
MEAN	0.58877	-0.19278	-0.24095
M1NCON	-0.19278	0.65904	0.68793
M2NCON	-0.24095	0.68793	0.83003

Table 3-1 (continued)

(4) Means and covariance matrix of normalized variables for training set: C. FLD 2

MEAN	-0.044681
M1NCON	0.035953
M2NCON	0.036922

	MEAN	M1NCON	M2NCON
MEAN	0.74096	0.08556	0.16471
M1NCON	0.08556	0.77133	0.25902
M2NCON	0.16471	0.25902	0.81482

(5) Means and covariance matrix of normalized variables for training set: C. FLD 3

MEAN	0.043122
M1NCON	0.039936
M2NCON	0.048926

	MEAN	M1NCON	M2NCON
MEAN	0.81140	-0.12739	0.21209
M1NCON	-0.12739	1.04026	0.64589
M2NCON	0.21209	0.64589	0.93263

(6) Means and covariance matrix of normalized variables for training set: VEGATATN

MEAN	-0.360367
M1NCON	-0.306482
M2NCON	-0.463614

	MEAN	M1NCON	M2NCON
MEAN	0.68209	0.52366	0.51271
M1NCON	0.52366	0.85514	0.87625
M2NCON	0.51271	0.87625	1.11746

(7) Means and covariance matrix of normalized variables for training set: SPORTS

MEAN	0.050055
M1NCON	0.069648
M2NCON	0.100605

	MEAN	M1NCON	M2NCON
MEAN	0.51072	0.19821	0.21475
M1NCON	0.19821	0.70298	0.57006
M2NCON	0.21475	0.57006	0.52075

(8) Means and covariance matrix of normalized variables for training set: PAVEMENT

MEAN	-0.047221
M1NCON	0.074504
M2NCON	0.083704

Table 3-1 (continued)

(8) (continued)

	MEAN	M1NCON	M2NCON
MEAN	0.53156	-0.45257	-0.45874
M1NCON	-0.45257	0.44403	0.44717
M2NCON	-0.45874	0.44717	0.45450

C. Confusion Matrix with the Training Sets Data

Step 1 Variables: MEAN M1NCON M2NCON

Rank of each set:

SOIL = 3 METAL = 3 C. FLD 1 = 3 C. FLD 2 = 3 C. FLD 3 = 3
PAVEMENT = 3 SPORTS = 3 VEGATATN = 3

CONFUSION MATRIX

	SOIL	METAL	C.FLD 1	C.FLD 2	C.FLD 3	VEGATATN	PAVEMENT	SPORTS
SOIL	285	0	0	0	0	1	4	10
METAL	0	296	0	0	0	2	0	2
C.FLD 1	0	0	90	22	0	6	0	3
C.FLD 2	0	0	83	338	0	18	0	1
C.FLD 3	0	0	0	0	188	72	0	0
VEGATATN	0	0	0	0	0	385	0	0
PAVEMENT	1	0	0	0	0	0	153	1
SPORTS	1	0	0	0	4	14	0	553

TOTAL CORRECT CLASSIFICATION = 90.33 PERCENT
ACTUAL CORRECT CLASSIFICATION = 94.79 PERCENT.

EXPLANATION: "Total"assumes each group is different. "Actual" ignors confusion between identically named groups (here, CF1, CF2 and CF3).

In summary, this new classifier based upon the stable distribution model consists of the following steps:

1. From the computed stable density function, a table of ratio values between percentiles is created according to a wide range of α and β values.

2. From this table, the stable parameters for each variable in each training set are estimated.

3. A monotonic non-linear function as described in Figure 3-1 is employed to transform each variable in each training set back to a more normal distribution with approximate mean zero and variance one.

4. Generation of confusion matrix using the training set data by means of the Mahalanobis classifier.

5. From each of the estimated stable distribution functions with the training sets data, the texture variables of each pixel in the test set are transformed into their normal equivalence.

6. Classification procedure utilized the same Mahalanobis classifier, i.e., using the minimum distance criterion (D^2).

7. Generate the decision map according to training sets and a rejected category.

8. Enumerate the percentage of each class from the decision map according to a (10 x 10) grid cells.

SECTION 4

DERIVATION OF A 3-VARIABLE TEXTURE EXTRACTOR AND ANALYSES OF IMAGE DATA

4.1 INTRODUCTION

The data set for this study is composed of seven scenes of the RADC's Northeast Test Area: Griffiss AFB, New York (GALA); Verona, New York, POL Storage (VPLA, VPHA): Stockbridge, New York, SAM site (SPLA, SBHA); and Utica, New York, Rail Yard (URLA), at both low altitude (LA) and high altitude (HA). In addition, two sub-scenes from a LANDSAT frame (Phoenix, Arizona) were also processed to test the applicability of the developed texture analysis to the LANDSAT data.

It should be noted that the training sets for the Phase-I effort were not the same as those for the analyses will be presented; and therefore, a direct comparison on the hit-rates is not appropriate. The change of the training sets was based on the fact that the training sets appeared optimal for the Gaussian model may not be appropriate for the stable distribution model.

4.2 A 3-VARIABLE TEXTURE EXTRACTOR FOR THE STABLE MAHALANOBIS CLASSIFIER

In Section 2.2.3 it was pointed out that we utilized all of the 17 texture variables in conjunction with the normal Mahalanobis classifier in pixel classification. By employing the stable distribution instead of the normal distribution as a model for the classifier, it was immediately evident that the needed number of texture variables in the classifier can be reduced to five, at most. The following illustrates this pattern.

TABLE 4-1. Texture Variable Patterns Associated With the Classifier Using VPLA Training Sets Data

A. Pattern 1 with these texture variables:

MEAN, STD DEV., M1NCON (1st neighbor contrast), M2NSQR (2nd neighbor contrast, squared)

Rank of each set:

SOIL = 4 METAL = 4 C.FLD 1 = 4 C.FLD 2 = 4 C.FLD 3 = 4
VEGATATN = 4 PAVEMENT = 4 SPORTS = 4

Table 4-1 (continued)

CONFUSION MATRIX

	SOIL	METAL	C.FLD 1	C.FLD 2	C.FLD 3	VEGATATN	PAVEMENT	SPORTS
SOIL	281	0	0	0	0	1	0	18
METAL	3	293	0	0	0	4	0	0
C.FLD 1	0	0	92	17	0	8	0	4
C.FLD 2	0	0	101	312	0	24	0	3
C.FLD 3	0	0	0	4	207	49	0	0
VEGATATN	0	0	0	1	0	384	0	0
PAVEMENT	2	0	0	0	0	0	152	1
SPORTS	0	0	0	0	4	35	0	533

TOTAL CORRECT CLASSIFICATION = 88.99 PERCENT.
ACTUAL CORRECT CLASSIFICATION = 94.24 PERCENT.

B. Pattern 2 with these texture variables:

MEAN, STD DEV., M1NCON (1st neighbor contrast), M2NCON (2nd neighbor contrast), MBDAT2 (area below datum 2)

Rank of each set:

SOIL = 5 METAL = 5 C.FLD 1 = 4 C.FLD 2 = 4 C.FLD 3 = 4

VEGATATN = 4 PAVEMENT = 5 SPORTS = 4

CONFUSION MATRIX

	SOIL	METAL	C.FLD L	C.FLD 2	C.FLD 3	VEGATATN	PAVEMENT	SPORTS
SOIL	269	0	0	0	0	1	0	30
METAL	0	287	0	0	0	2	0	11
C.FLD 1	0	0	93	17	0	8	0	3
C.FLD 2	0	0	90	328	0	19	0	3
C.FLD 3	0	0	0	1	200	59	0	0
VEGATATN	0	0	0	0	0	385	0	0
PAVEMENT	0	0	0	0	0	5	149	1
SPORTS	0	0	0	0	4	37	0	531

TOTAL CORRECT CLASSIFICATION = 88.51 PERCENT.
ACTUAL CORRECT CLASSIFICATION = 93.17 PERCENT.

C. Pattern 3 with these texture variables:

MEAN, STD DEV., M1NCON (1st neighbor contrast), M2NCON (2nd neighbor contrast), MBDAT1 (area below datum 1)

Rank of each set:

SOIL = 4 METAL = 5 C.FLD 1 = 4 C.FLD 2 = 4 C.FLD 3 = 4

VEGATATN = 4 PAVEMENT = 5 SPORTS = 5

Table 4-1 (continued)

CONFUSION MATRIX

	SOIL	METAL	C.FLD 1	C.FLD 2	C.FLD 3	VEGATATN	PAVEMENT	SPORTS
SOIL	281	0	0	0	0	18	1	0
METAL	4	289	0	0	0	7	0	0
C.FLD 1	0	0	93	17	0	6	0	5
C.FLD 2	0	0	89	327	0	18	0	6
C.FLD 3	0	0	0	1	200	59	0	0
VEGATATN	0	0	0	0	0	385	0	0
PAVEMENT	2	0	0	0	0	5	148	0
SPORTS	2	0	0	0	4	39	0	527

TOTAL CORRECT CLASSIFICATION = 88.83 PERCENT.
ACTUAL CORRECT CLASSIFICATION = 93.64 PERCENT.

D. Pattern 4 with these texture variables:

MEAN, STD DEV., M1NCON (1st neighbor contrast), M2NCON (2nd neighbor contrast), MADAT2 (area above datum 2)

Rank of each set:

SOIL = 4 METAL = 4 C.FLD 1 = 4 C.FLD 2 = 4 C.FLD 3 = 4

VEGATATN = 4 PAVEMENT = 5 SPORTS = 4

CONFUSION MATRIX

	SOIL	METAL	C.FLD 1	C.FLD 2	C.FLD 3	VEGATATN	PAVEMENT	SPORTS
SOIL	283	0	0	0	0	2	0	15
METAL	3	290	0	0	0	2	0	5
C.FLD 1	0	0	93	17	0	8	0	3
C.FLD 2	0	0	89	329	0	19	0	3
C.FLD 3	0	0	0	1	200	59	0	0
VEGATATN	0	0	0	0	0	385	0	0
PAVEMENT	5	0	0	0	0	1	148	1
SPORTS	2	0	0	0	4	37	0	529

TOTAL CORRECT CLASSIFICATION = 89.10 PERCENT.
ACTUAL CORRECT CLASSIFICATION = 93.72 PERCENT.

E. Pattern 5 with these texture variables:

MEAN, STD DEV., M1NCON (1st neighbor contrast), M2NCON (2nd neighbor contrast), MADAT1 (area above datum 1)

Rank of each set:

SOIL = 4 METAL = 4 C.FLD 1 = 4 C.FLD 2 = 4 C.FLD 3 = 4

VEGATATN = 5 PAVEMENT = 4 SPORTS = 5

Table 4-1 (continued)

CONFUSION MATRIX

	SOIL	METAL	C.FLD 1	C.FLD 2	C.FLD 3	VEGATATN	PAVEMENT	SPORTS
SOIL	277	0	0	0	0	0	1	22
METAL	1	294	0	0	0	0	0	5
C.FLD 1	0	0	96	17	0	8	0	0
C.FLD 2	0	0	88	318	0	34	0	0
C.FLD 3	0	0	0	0	182	78	0	0
VEGATATN	8	0	0	0	0	376	0	1
PAVEMENT	1	0	0	0	0	0	150	4
SPORTS	2	0	0	0	4	62	0	504

TOTAL CORRECT CLASSIFICATION = 86.74 PERCENT.
ACTUAL CORRECT CLASSIFICATION = 91.04 PERCENT.

F. Pattern 6 with these texture variables:

MEAN, STD DEV., M1NCON (1st neighbor contrast), M2NCON (2nd neighbor contrast), MADAT 3 (area above datum 3)

Rank of each set:

SOIL = 5 METAL = 5 C.FLD 1 = 4 C.FLD 2 = 4 C.FLD 3 = 4

VEGATATN = 4 PAVEMENT = 5 SPORTS = 4

CONFUSION MATRIX

	SOIL	METAL	C.FLD 1	C.FLD 2	C.FLD 3	VEGATATN	PAVEMENT	SPORTS
SOIL	285	0	0	0	0	2	1	12
METAL	0	296	0	0	0	1	0	3
C.FLD 1	0	0	93	17	0	8	0	3
C.FLD 2	0	0	89	329	0	19	0	3
C.FLD 3	0	0	0	1	200	59	0	0
VEGATATN	0	0	0	0	0	385	0	0
PAVEMENT	0	0	0	0	0	1	151	3
SPORTS	1	0	0	0	4	37	0	530

TOTAL CORRECT CLASSIFICATION = 89.58 PERCENT.
ACTUAL CORRECT CLASSIFICATION = 94.20 PERCENT.

G. Pattern 7 with these texture variables:

MEAN, STD DEV., M1NCON (1st neighbor contrast), M2NCON (2nd neighbor contrast), MBDAT3 (area below datum 3)

Rank of each set:

SOIL = 5 METAL = 5 C.FLD 1 = 4 C.FLD 2 = 4 C.FLD 3 = 4

VEGATATN = 4 PAVEMENT = 5 SPORTS = 4

Table 4-1 (continued)

CONFUSION MATRIX

	SOIL	METAL	C.FLD 1	C.FLD 2	C.FLD 3	VEGATATN	PAVEMENT	SPORTS
SOIL	283	0	0	0	0	1	1	15
METAL	1	294	0	0	0	2	0	3
C.FLD 1	0	0	93	17	0	8	0	3
C.FLD 2	0	0	90	328	0	19	0	3
C.FLD 3	0	0	0	1	200	59	0	0
VEGATATN	0	0	0	0	0	385	0	0
PAVEMENT	1	0	0	0	0	2	150	2
SPORTS	0	0	0	0	4	37	0	531

TOTAL CORRECT CLASSIFICATION = 89.38 PERCENT.
ACTUAL CORRECT CLASSIFICATION = 94.04 PERCENT.

H. Pattern 8 with texture variables:

MEAN, M1NCON, M2NCON

Rank of each set:

SOIL = 3 METAL = 3 C.FLD 1 = 3 C.FLD 2 = 3 C.FLD 3 = 3

VEGATATN = 3 PAVEMENT = 3 SPORTS = 3

CONFUSION MATRIX

	SOIL	METAL	C.FLD 1	C.FLD 2	C.FLD 3	VEGATATN	PAVEMENT	SPORTS
SOIL	285	0	0	0	0	1	4	10
METAL	0	296	0	0	0	2	0	2
C.FLD 1	0	0	90	22	0	6	0	3
C.FLD 2	0	0	83	338	0	18	0	1
C.FLD 3	0	0	0	0	188	72	0	0
VEGATATN	0	0	0	0	0	385	0	0
PAVEMENT	1	0	0	0	0	0	153	1
SPORTS	1	0	0	0	4	14	0	553

TOTAL CORRECT CLASSIFICATION = 90.33 PERCENT.
ACTUAL CORRECT CLASSIFICATION = 94.79 PERCENT.

Pattern 1 shows that four texture variables were used in the classifier for computing the hit-rate of the VPLA training sets. The choise of these variables were based on the following reasoning:

(1) Since "MEAN" and "STANDARD DEVIATION" are the most basic texture tone variables, they were entered in the analysis first.

(2) Since texture is generally defined as spatial distribution of tones, the "1st neighbor contrast" was a logical candidate.

(3) "2nd neighbor contrast squared" was utilized here because the 2nd order statistics was proved to be effective in visual discrimination of textures (Julesz, 1975).

Pattern 2 was intended to bring up the hit-rate by using five texture variables instead of four, where "the 2nd neighbor contrast" replaced "2nd neighbor contrast squared," and "area below datum 2 (tone level of 100)" was added to the list.

By comparing the hit-rate figures, it was noticed immediately, to our surprise, that the hit-rate went down with an increase of an additional texture measure.

Pattern 3 is an experiment almost identical to Pattern 2 except "area below datum 1 (tone level 50)" replace "area below datum 2." The hit-rate was still below 94 percent, although slightly better than that of Pattern 2.

Pattern 4 through pattern 7 are variations of patterns 2 and 3. The experiments were designed to evaluate the effectiveness of the variables related to areas above and below 3 given datum planes (50, 100, 150), which have been proved to be highly effective in conjunction with the normal Mahalanobis classifier for our Phase-I effort.

It should be noted here that none of these 5-variable systems were performing better than the original 4-variable systems given in Pattern 1 with a hit-rate of 94.24 percent.

The final experiment, Pattern 8, was intended to evaluate how the classifier would behave if one utilized only 3 variables instead of 4 (Pattern 1) or 5 (Pattern 2 through Pattern 7). Again, to our surprise, the hit-rate went up (to 94.79 percent) instead of going down. From these experiments, we are able to draw the following conclusion regarding the stable Mahalanobis classifier:

1. As compared to the Gaussion model, stable distribution model, upon which the classifier is developed needs much less number of variables in the feature extractor. This can be attributed to the factor that there are already four parameters (location,

scale, stable index, and symmetry parameter) in the stable classifier instead of two (mean and standard deviation) in the normal model.

2. It appears that the stable classifier prefers variables made of 1st order statistics, such as 1st neighbor contrast, and dislikes wave-form parameters such as area above and below datum planes, which are highly effective for the normal model.
3. The optimal number of variables seems to lie between 3 and 5, and in many cases 3 is optimal.
4. The best texture variables for the stable classifier seem to be (1) mean, (2) 1st neighbor contrast, and (3) 2nd neighbor contrast.

4.3 GENERATION OF DECISION MAPS AND HIT-RATE ANALYSIS

4.3.1 The Classification Logic

It bears repeating that the classification logic of the classifier utilizes a minimum distance (Mahalanobis D^2) criterion as follows:

$D_i^2 = (Y - U_i)^t (Q_i)^-(Y - u_i)$ (as of Equation (1))

where

Y is the texture vector of the unknown pixels

U_i is the centroid of each training set

Q_i is the dispersion matrix of each training set

T stands for transpose of a matrix

(-) stands for the generalized inverse of a matrix

and then assign Y to population i if $D_i^2 = \min \{D_1^2, \ldots, D_k^2\}$

Since we utilized a normal transformation of the stable distribution parameters in the above equation for the training sets data, the transformed values (texture vector) of Y (unknown pixels) instead of the raw scores must also be utilized in the classification process with Equation (1). The transformation process of the test set data follows the same procedures explained in Figure 3-1.

Again, since D^2's have an χ^2 distribution, a reject category can be established according to the probability levels that each pixels would belong to a given training set. In other words, a cut-off probability level, say, 0.01 or 0.02 can be used to establish a reject class.

4.3.2 Analyses of the Data Sets

Utilizing the same data sets (VPLA, GALA, SBLA, URLA, VPHA, GAHA and SBHA) of this Phase-I effort, seven decision maps were generated using the new classifier based on the stable distribution model as follows.

Table 4-2 shows a series of hit-rate analyses. Unlike the Phase-I effort, the hit-rate analyses have removed the effect of "rejects", that is, the analysis is carried out with the classified data alone. The problem of "rejects" will be discussed in detail in Section 5 regarding automatic selection of training sets.

TABLE 4-2. Hit-rate Analyses

A. The VPLA Frame (rejects: 23.79%)

Terrain Types	Decision Map (%)	Photo-Interpretation (%)	Hit-rate
Vegetation	6.62	6.71	99%(1.35)
Cultivated Fields	33.75	32.37	96% (4.27)
Soil	28.46	30.74	93% (7.42)
Metal	1.01	1.21	83% (16.53)
Pavement	6.37	5.15	76% (23.69)

B. The GALA Frame (rejects: 13.48%)

Terrain Types	Decision Map (%)	Photo-Interpretation (%)	Hit-rate
Vegetation	3.77	4.79	79%
Cultivated Fields	60.53	55.14	90%
Metal	0.49	0.64	90%
Soil	5.90	5.85	99%
Pavement	15.83	19.44	81%

C. The SBLA Frame (rejects: 21.47%)

Terrain Types	Decision Map (%)	Photo-Interpretation (%)	Hit-rate
Vegetation	49.53	40.66	80%
Cultivated Field	28.81	21.67	99%
Soil	21.49	16.43	90%

D. The URLA Frame (rejects: 0.97%)

Terrain Types	Decision Map (%)	Photo-Interpretation (%)	Hit-rate
Soil	4.40	6.34	70%
Pavement	31.46	28.49	90%
*Metal	8.71	4.30	
Urban	7.84	9.61	82%
Composition	46.63	51.26	91%

*Original figure is 17.11% with 1% digitization error.

Table 4-2 (continued)

E. The VPHA Frame (rejects: 3.94%)

Terrain Types	Decision Map (%)	Photo-Interpretation (%)	Hit-Rate
Pavement	6.69	3.57	13%
Vegetation	14.32	15.59	92%
Cultivated Fields	46.69	56.88	82%
Soil	*16.11	16.63	97%
Composition	11.25	8.31	65%

F. The GAHA Frame (Rejects:

Terrain Types	Decision Map (%)	Photo-Interpretation (%)	Hit-Rate
Vegetation and Cultivated Field	66.22	70.81	94%
Soil	6.57	7.91	84%
Pavement	7.25	5.55	70%
Composition	17.26	15.73	91%

G. The SBHA Frame (rejects: 4.08%)

Terrain Types	Decision Map (%)	Photo-Interpretation (%)	Hit-Rate
Vegetation	15.12	17.86	85%
Cultivated Fields	57.47	53.55	93%
Composition	7.05	8.85	80%
Soil	16.28	16.93	97.2%
Other (water & pave)	0	2.81	

*Original figure is 17.11% with 1% digitization error.

4.4 CONCLUDING REMARKS ON THE STABLE MAHALANOBIS CLASSIFIER

By observing the performance of both normal and stable Mahalanobis classifiers, the following remarks can be used as a general, comparative analysis.

1. Compared to the normal model, the stable classifier is more sensitive to the distributional characteristic of the training sets. Specifically, bimodel or similar distributions (mixture of classes) can create a much larger amount of misclassifications with the stable classifier.
2. Because of (1), pre-processing of the training sets data in many occasions is a necessary procedure for the stable classifier. Once this is done, the stable classifier performs very well.
3. The stable classifier tends to reduce the amount of "rejects." This can be attributable to the fact that the stable model has fatter tails.
4. Since the training sets for the Phase-I effort and the Phase-II effort were not identical, a direct comparison between the hit-rates (i.e., Table 24 versus Table 4-2) *should not be made.* In general, we feel that the stable model performed slightly better than the normal model, especially in the high altitude frames.
5. We feel the real gain in using the stable classifier is the data processing rate--a factor six times faster has been obtained. That is, since the stable model needs only three texture feature variables in the classifier, the processing time of (256 x 256) pixels has been reduced to 18 minutes from 90 minutes of CPU time, where IBM 370-158 computer with FORTRAN language, and the normal classifier using 17 feature variables was utilized during the Phase-I effort.

SECTION 5

AUTOMATIC SELECTION OF TRAINING SETS WITH TEXTURE ANALYSIS

5.1 INTRODUCTION

In our Phase-I and Phase-II studies of feature extraction, the most serious problem in decision maps is the large amount of rejects, or unclassified pixels. In a strict sense, they should be treated as errors. Since these rejects represent classes other than the selected training sets, they can be reduced to an insignificant amount by introducing additional training sets in the analysis provided that these new training sets can truly represent the unclassified pixels.

To be successful in selecting manually appropriate (enough) training sets, the analyst usually has to repeat the analysis many times until the amount of rejects is acceptable. Two drawbacks can be noted here:

(1) it is a slow method of image processing; and

(2) one cannot be sure that all of the needed training sets can be selected manually with visual inspection of tonal (primarily) difference of pixels.

In this section, we will present an alternative procedure for the selection of training sets, and evaluate it by comparing the decision maps (hit-rate analysis) against those presented in Section 4.

5.2 SYSTEMATIC SAMPLING COUPLING WITH CLUSTERING ANALYSIS AS A METHOD FOR AUTOMATIC SELECTION OF TRAINING SETS

To include all the necessary training sets in the decision map, the best solution is to first sample randomly pixels from the test set (frame), and then group them into distinctive classes, from which the desired training sets can be selected. In our experiments, we employed a systematic sampling method; that is, every 30th pixel was selected from the frame (256 x 256) and yielded a sample of 2111 pixels.

We will then cluster these 2116 points into distinctive groups step by step using the three texture variables (mean, 1st neighbor contrast, and 2nd neighbor contrast). The developed clustering algorithm utilizes two stages of grouping process: the first stage will quickly group 2111 points into about 200 classes with a nearest neighbor criterion, and the second stage will slowly group them further into only a few classes with a method similar to the Mahalanobis classifier. Table 5-1 illustrates this grouping method using GALA as an example.

TABLE 5-1. Clustering Pattern of Sampled Pixels With Texture Analysis

A. Summary of Texture Clustering Analysis

Reverse leader cluster analysis of 2116 cases.

A switch to a slower but better clustering algorithm occurs at 200 clusters or less.

The variables are weighted as follows (normalized weights):
1: 0.4623 2: 1.3887 3: 0.9258 (1 = mean brightness, 2 = 1st neighbor contrast, 3 = 2nd neighbor contrast).

PASS	CLUSTERS	SPECIFIED RADIUS	CLOSEST LEADERS	MAX. GROUP RADIUS	EFFECTIVE RADIUS
1.	722	1.000	1.001	0.99982	1.000
2.	302	2.002	2.000	1.99963	3.002
3.	102	4.011	4.028	4.00657	7.013
4.	33	8.056	8.080	8.00264	15.068
5.	12	16.161	17.233	15.82734	31.229
6.	6	34.466	35.505	33.10715	65.695

B. 33 Group With Mean and SD of the Texture Variables

	1 (tone)	2 (1st neighbor contrast)	3 (2nd neighbor contrast)
1.	55.8769 (6.71132)	2.6929 (0.88393)	3.8397 (1.84229)
2.	88.5459 (10.55251)	3.7731 (1.26970)	5.7352 (2.77562)
3.	135.5946 (8.39666)	10.7598 (1.40650)	20.5785 (2.92008)
4.	36.2701 (6.99684)	2.4002 (0.80505)	3.3666 (1.66419)
5.	98.6189 (2.17137)	13.2857 (2.24726)	25.5714 (3.47859)
6.	109.8158 (11.99365)	8.1904 (1.30287)	14.6926 (3.01707)
7.	148.1694 (9.59044)	6.4426 (1.70876)	12.2037 (3.11850)

Table 5-1 (continued)

	1 (tone)	2 (1st neighbor contrast	3 (2nd neighbor contrast)
8.	111.2636 (4.34858)	11.8750 (1.11807)	21.5831 (2.49731)
9.	172.0554 (3.28110)	22.9165 (0.83371)	45.8335 (1.66646)
10.	76.4430 (6.64707)	9.2808 (2.17041)	17.6522 (4.36359)
11.	163.9532 (8.82955)	2.9967 (0.81972)	4.4789 (1.95284)
12.	124.0555 (5.83330)	18.1250 (1.20788)	36.2500 (2.41698)
13.	315.0559 (4.50217)	15.4165 (0.08405)	30.6665 (0.33439)
14.	241.7406 (3.12375)	2.1387 (0.07874)	3.4997 (0.47140)
15.	56.5714 (7.90837)	6.1429 (1.57419)	10.9564 (3.42151)
16.	47.9490 (5.13599)	8.2691 (1.44509)	15.1952 (1.90770)
17.	230.1775 (2.42061)	9.0332 (0.79690)	17.4000 (1.96260)
18.	191.0000 (0.0)	26.5830 (0.0)	51.8330 (0.0)
19.	174.3330 (0.0)	30.0830 (0.0)	60.1670 (0.0)
20.	119.4861 (4.15801)	6.6250 (1.10556)	8.6667 (1.80850)
21.	135.5560 (0.0)	29.8330 (0.0)	59.6670 (0.0)
22.	137.8889 (5.89094)	23.8335 (0.58380)	47.0000 (1.83286)
23.	58.3254 (7.23915)	12.3690 (0.97845)	24.3096 (1.99774)
24.	81.8517 (3.17707)	14.8053 (1.28617)	27.0557 (1.22743)
25.	93.1945 (4.93473)	10.6250 (0.88300)	10.6665 (2.34212)
26.	77.0988 (5.58108)	16.4334 (0.94657)	37.8666 (1.89250)
27.	137.2665 (4.86096)	3.6722 (0.82851)	6.0333 (1.39194)
28.	28.9124 (7.66667)	5.3033 (1.01738)	9.4786 (2.22820)
29.	127.3999 (1.36502)	13.6500 (0.69825)	27.0334 (1.67771)
30.	176.3334 (5.25372)	6.7710 (0.54773)	13.2915 (1.20963)
31.	117.6670 (0.0)	21.9170 (0.0)	43.8330 (0.0)
32.	11.8147 (4.83124)	2.2386 (0.76926)	3.3308 (1.49248)
33.	11.5927 (4.70538)	6.5553 (1.37509)	10.8890 (3.37262)

Table 5-1 (continued)

C. 12 Groups with Mean and SD of the Texture Variables

Their association with the ground truth are interpreted by using the manually selected training sets data given in D (next page).

Means (and standard deviations) of each variable for each group after pass 5.

	1	2	3	No. of Pixels	Probable Ground Truth
1.	67.0821 (15.74348	3.0069 (1.53175)	4.5336 (3.15977)	1525	Cultivated fields (1)
2.	143.4283 (11.38787)	8.0758 (2.90480)	15.4353 (5.71575	67	Soil (2)
3.	98.3820 (15.71126)	14.0333 (2.55333)	26.7865 (5.51332)	25	Edge-pave
4.	93.9785 (19.44955)	8.6935 (1.91241)	15.7245 (4.32168)	170	Soil (1)
5.	164.2036 (20.08715)	25.0277 (2.63984)	49.6112 (5.33552)	6	Pave (2)
6.	161.5503 (11.94159)	3.1695 (1.03471)	4.8801 (2.40241)	146	Pave (1)
7.	225.9570 (7.52703)	10.8570 (2.96163)	21.1904 (6.22111)	7	Metal
8.	241.7406 (3.12375)	2.1387 (0.07874)	3.4997 (0.47140)	3	(isolated cases)
9.	29.0771 (14.05051)	7.3889 (2.69996)	13.6396 (5.47333)	99	Cultivated fields (3)
10.	135.5560 (0.0)	29.8330 (0.0)	59.6670 (0.0)	1	(isolated cases)
11.	117.6670 (0.0)	21.9170 (0.0)	43.8330 (0.0)	1	(isolated cases)
12.	11.8147 (4.83124)	2.2386 (0.76926)	3.3308 (1.49248)	36	Vegetation

Table 5-1 (continued)

D. Ground Truth Information Obtained by using Manual Methods

Ground truth information

Location, scale, alpha and beta for each possible variable in each training set.

	Pavement	C. Fld 1	C. Fld 2	C. Fld 3	Vegatatn	Metal	Soil 1	Soil 2	Edgepav5
MEAN	166.82787	42.47398	54.96819	26.52441	10.22213	215.48701	106.95882	100.37669	97.20404
	3.74690	1.61669	0.84133	2.58790	2.16672	11.92308	4.08394	2.52299	6.49971
	1.90	1.80	1.60	1.50	1.80	1.30	1.60	1.50	1.80
	1.00	-1.00	0.80	0.90	1.10	-1.00	-1.00	-1.00	0.60
M1NCON	2.84566	2.13741	1.77579	2.17799	2.58746	12.71855	6.64512	4.69820	7.97275
	0.65865	0.43957	0.38185	0.41737	0.45856	5.67634	2.10051	0.99443	3.36382
	1.90	1.90	1.70	1.90	1.60	1.40	1.60	1.50	1.90
	1.00	0.60	1.00	0.90	0.90	0.90	1.00	0.80	0.60
M2NCON	4.48477	2.45891	2.11607	2.83634	3.61934	22.90981	12.96803	7.85736	15.44399
	1.64528	0.70291	0.53430	0.84872	1.13459	11.95163	4.78067	1.68430	6.27913
	1.80	1.90	1.60	1.70	1.80	1.50	1.60	1.30	1.70
	1.00	1.00	0.60	1.00	0.70	1.00	1.00	0.70	1.00

Note: When $\alpha = 2$ and $\beta = 0$, the distribution is normal. The numbers in C and D would match only when $\alpha = 2$ and $\beta = 0$; otherwise, slight variations should be allowed for making comparisons.

In Figure 5-1, A shows the number of clusters obtained in each iteration (pass), B indicates the 33 distinctive clusters characterized by the texture variables after four iterations, and C is similar to B, but indicates only 12 clusters. By using the ground truth information as indicated in D, we identified the terrain types for clusters shown in C.

5.3 ANALYSIS OF THE TRAINING SETS DATA AND GENERATION OF DECISION MAPS

By examining the number of pixels in each cluster and the characteristics of the texture variables representing the clusters, we then selected ten training sets from the 33 clusters in pass 5 as indicated in Figure 5-1, C.

Table 5-2 is a hit-rate analysis with the training sets.

TABLE 5-2. Confusion Matrix of the Training Sets

Texture Variables: MEAN M1NCON M2NCON

Rank of each set: CLUSTR 1 = 3 CLUSTR 2 = 3 CLUSTR 4 = 3 CLUSTR 6 = 3 CLUSTR 10 = 3
CLUSTR 11 = 3 CLUSTR 16 = 3 CLUSTR 17 = 3 CLUSTR 31 = 3 CLUSTR 32 = 3

CONFUSION MATRIX

	CLUSTR 1	CLUSTR 2	CLUSTR 4	CLUSTR 6	CLUSTR 10	CLUSTR 11	CLUSTR 16	CLUSTR 17	CLUSTR 31	CLUSTR 32
CLUSTR 1	467	8	13	3	15	0	14	0	0	0
CLUSTR 2	0	73	0	9	3	0	0	0	0	0
CLUSTR 4	22	0	695	4	0	0	3	6	7	5
CLUSTR 6	0	4	0	67	9	0	0	0	0	0
CLUSTR 10	1	0	0	2	77	0	4	0	0	0
CLUSTR 11	0	0	0	0	0	151	0	0	0	0
CLUSTR 16	0	0	0	1	2	0	135	3	0	0
CLUSTR 17	0	0	0	0	0	0	8	46	0	0
CLUSTR 31	0	0	2	0	0	0	0	0	51	0
CLUSTR 32	0	0	1	0	0	0	0	0	3	58

Total Correct Classification = 91.87 percent.
Actual Correct Classification = 91.87 percent.

MAHALANOBIS DISTANCES FROM ROW SET TO COLUMN SET

	CLUSTR 1	CLUSTR 2	CLUSTR 4	CLUSTR 6	CLUSTR 10	CLUSTR 11	CLUSTR 16	CLUSTR 17	CLUSTR 31	CLUSTR 32
CLUSTR 1	0.1	7.1	22.5	15.1	12.6	11.5	7.6	14.7	27.3	22.2
CLUSTR 2	14.8	0.0	23.3	7.0	14.9	17.2	28.7	45.3	28.7	22.0
CLUSTR 4	12.5	27.0	0.3	31.2	31.6	26.7	17.8	8.1	7.6	5.7
CLUSTR 6	10.7	6.5	12.3	0.1	4.4	33.3	6.7	7.2	11.8	13.7
CLUSTR 10	10.3	6.6	26.2	8.5	0.0	20.8	10.9	20.4	24.2	26.5
CLUSTR 11	10.6	8.5	11.8	12.3	15.7	0.1	14.1	15.5	11.6	13.8
CLUSTR 16	10.5	28.0	28.0	22.4	13.1	22.1	0.3	4.0	10.6	35.3
CLUSTR 17	51.3	114.8	16.8	48.7	21.3	123.6	12.8	0.1	7.5	14.8
CLUSTR 31	27.6	21.8	15.4	20.1	20.6	21.6	18.0	11.9	0.4	6.7
CLUSTR 32	25.8	31.6	24.7	46.6	46.6	28.4	46.6	46.6	14.1	0.1

We determined that the hit-rate of the training sets data as shown in Table 5-2 was high enough, and then proceeded to generate a decision map using the test set (GALA). The hit-rate analysis of the decision map is given in Table 5-3.

TABLE 5-3. Hit-rate Analysis of the Test Set (rejects: 0%)

	Computer Decision Result	Photo-interpretation	Hit-rate
Vegetation	5.79%	5.01%	85%
Cultivated field	67.77%	61.87%	91%
Soil	5.98%	6.94%	87%
Pavements	17.73%	23.87%	75%
Metal	2.73%	2.31%	82%
Total	100.00%	100.00%	

5.4 COMPARISON BETWEEN MANUAL AND AUTOMATIC SELECTION OF TRAINING SETS IN THE CONTEXT OF HIT-RATES IN TEST SETS

In general, we feel that the automatic selection of training sets is a superior method to the manual operation with a cursor. This conclusion is based on three experiments (GALA, VPLA, SBLA), where the amount of rejects was reduced to an insignificant percentage, and at the same time the overall hit-rates in the test sets remained as high as those obtained by using the manually selected training sets data. Table 5-4 gives the experimental results.

5.5 TEXTURE ANALYSIS OF LANDSAT DATA

It was often assumed that there is no texture information in LANDSAT data because of their poor resolution (i.e., about one acre per pixel). Mr. Bush of RADC asked us to look into the applicability of LANDSAT data for terrain classification with texture analysis. The experiments for this purpose utilized a LANDSAT tape of Phoenix, Arizona.

From IBM Corporation, we obtained a print (positive) of Band 4 of the Phoenix frame for the ground truth and locational controls of the experimental sub-scenes. Since the image print of Band 4 is at the scale of about 1:500,000, the area of a sub-scene composed of (256 x 256) pixels

TABLE 5-4. Comparison of Hit-rates in Test Sets: Automatic Training Sets Versus Manual Training Sets

A. Hit-rates in GALA frame

	Terrain Types	With Automatic Training Sets	With Manual Training Sets
	Rejects	0%	13.48%
1.	Vegetation	85%	79%
2.	Cultivated Field	91%	90%
3.	Soil	87%	99%
4.	Pavement	75%	81%
5.	Metal	82%	90%

B. Hit-rates in VPLA frame

	Terrain Types	With Automatic Training Sets	With Manual Training Sets
	Rejects	3.05%	23.79%
1.	Vegetation	97%	99%
2.	Cultivated Field	99%	96%
3.	Soil	99%	93%
4.	Pavement	96%	76%
5.	Metal	(not included)	83%

C. Hit-rates in SBLA frame

	Terrain Types	With Automatic Training Sets	With Manual Training Sets
	Rejects	2.55%	21.47%(Table 4-2)
1.	Vegetation	97%	80%
2.	Cultivated Field	99%	99%
3.	Soil	88%	90%

will be only (1 inch)^2. To make the sub-scene become (2 inch)^2, we averaged 4 pixels into one unit. This means the original tape of approximately (4000 x 4000) became (2000 x 2000) pixels; and therefore the resolution is four acres on the ground.

Utilizing the same sampling method (i.e., every 30th pixel), we cluster the sampled data distinctive groups according to a stepwise iteration pass. The train sets were then selected from one of the passes. In the following example, we selected 14 groups from the 41 clusters at pass 10. Table 5-5 shows the texture characteristics of each cluster in pass 10.

From this table, it is evident that there exists texture information in LANDSAT data even at the resolution level of four acres per pixel. For instance, if we take cluster 10 and cluster 19 for a comparison, we can see that in Band 4, the tone is almost the same (89.39 vs 89.34); however, the 1st neighbor contrast in cluster 19 is 1.5 times as much as that of cluster 10 (6.01 vs 3.91). Again, in Band 7, we see the spatial contrast in cluster 5 is almost twice as much as that of cluster 14 (i.e., 30.22 vs 17.22), whereas the tonal difference between them is insignificantly small (147 vs 156). Therefore, it can be fairly concluded that texture features in LANDSAT data provided enough information for terrain classification, specifically when multiple bands are used simultaneously in the analysis.

From the 41 clusters in pass 10, we then selected 14 clusters as the training sets. A hit-rate analysis was then performed to determine the power of the tone-texture information for class separation. Table 5-6 is a confusion matrix of the training sets with a hit-rate of 79.88 percent. The actual correct classification rate should be much higher when some of the clusters are grouped together according to ground truth information.

We also generated a decision map using 14 training sets. It can be concluded from a comparison between the decision map and the image (positive) pattern that the classification result is highly successful, and therefore, LANDSAT data can be used for terrain classification purposes with the developed texture analysis/automatic selection of training sets procedure.

TABLE 5-5. Texture Characteristics of LANDSAT Data

Texture Variables: Tone and 1st neighbor contrast in Bands 4, 5 and 7.

Means (and standard deviations) of each variable for each group after pass 10.

		1	2	3
	No. of Pixels	Tone of Band 4	1st Neighbor Contrast of Band 4	Tone of Band 5
1.	720	169.8312 (10.86458)	7.0942 (3.05008)	171.4559 (17.26991)
2.	78	145.5412 (9.05193)	15.6045 (6.78964)	132.4359 (13.26620)
3.	18	108.6111 (9.64669)	9.8287 (3.71707)	71.4752 (18.83240)
4.	152	121.4324 (15.23244)	15.9741 (5.99467)	90.3727 (28.38057)
5.	75	103.4331 (7.73865)	11.7933 (4.17626)	54.8235 (14.21441)
6.	133	140.0993 (12.97263)	21.9278 (5.37600)	123.5940 (23.55977)
7.	102	135.0235 (11.15866)	9.2286 (4.92354)	117.3178 (18.33138)
8.	165	153.8744 (11.08772)	15.6782 (3.91444)	149.1193 (19.29419)
9.	5	138.9330 (13.85979)	7.6834 (4.66358)	121.8001 (16.47690)
10.	19	89.3976 (4.24908)	3.9124 (1.85067)	31.3859 (6.79222)
11.	32	104.8923 (13.41189)	12.5079 (4.68618)	55.9339 (24.78380)
12.	15	102.1406 (6.23999)	13.1999 (3.63540)	52.5481 (12.39665)
13.	398	178.9224 (10.58430)	7.0229 (3.63869)	197.6653 (15.69883)
14.	25	117.8310 (9.06552)	19.7398 (3.80378)	83.6577 (15.86762)
15.	26	123.1708 (9.38999)	22.1344 (3.96210)	90.7606 (17.06926)
16.	16	131.9095 (8.97523)	7.5625 (3.40600)	117.3331 (14.50404)
17.	19	104.6255 (14.91303)	9.5350 (4.71361)	57.6140 (22.36143)
18.	13	113.1794 (14.52207)	6.2628 (3.05470)	79.7518 (30.56595)
19.	18	89.3456 (4.76847)	6.0139 (2.59468)	28.7961 (6.68553)
20.	13	171.3245 (9.48704)	24.5000 (3.50303)	175.0681 (11.81481)
21.	5	124.2665 (4.10173)	7.3002 (1.95269)	104.3553 (5.66065)
22.	1	144.8890 (0.0)	11.5000 (0.0)	129.2220 (0.0)
23.	10	90.0556 (4.30661)	4.1000 (1.31549)	29.7332 (10.24227)
24.	1	99.4440 (0.0)	5.3330 (0.0)	47.4440 (0.0)
25.	2	143.2780 (10.50037)	12.7500 (2.25002)	129.7775 (3.66732)
26.	5	116.0441 (9.92767)	11.0664 (1.80998)	78.9775 (15.91174)
27.	3	95.1106 (2.86888)	8.4167 (2.56103)	39.9260 (6.70138)
28.	15	132.0296 (6.20820)	24.5277 (2.22166)	106.7776 (9.10872)

Table 5-5 (continued)

	No. of Pixels	1 Tone of Band 4	2 1st Neighbor Contrast of Band 4	3 Tone of Band 5
29.	6	90.9257 (5.85435)	6.3193 (2.76595)	32.8703 (9.45749)
30.	2	128.1110 (3.22224)	34.1670 (0.50000)	99.3330 (12.00000)
31.	4	195.2778 (0.78561)	14.5417 (4.01414)	187.9443 (15.76661)
32.	1	169.8890 (0.0)	31.8330 (0.0)	145.0000 (0.0)
33.	3	160.3705 (6.57558)	6.4443 (2.22586)	156.1479 (7.23085)
34.	1	220.2220 (0.0)	12.4170 (0.0)	81.1110 (0.0)
35.	4	189.8609 (2.42626)	6.2915 (3.19530)	208.3609 (7.31357)
36.	2	185.8329 (1.39754)	23.9165 (3.58348)	196.6110 (1.16257)
37.	2	184.2775 (0.93750)	7.2915 (1.45850)	207.0554 (0.29315)
38.	1	208.4440 (0.0)	9.5830 (0.0)	207.6670 (0.0)
39.	2	160.3889 (1.83924)	33.3750 (0.54262)	135.4445 (9.44474)
40.	1	169.2220 (0.0)	35.8330 (0.0)	112.3330 (0.0)
41.	2	227.6669 (1.12500)	11.3335 (1.91650)	88.3890 (23.38904)

	No. of Pixels	4 1st Neighbor Contrast of Band 5	5 Tone of Band 7	6 1st Neighbor Contrast of Band 7
1.	720	12.1096 (5.45118)	85.4012 (24.82863)	14.0380 (6.41015)
2.	78	26.4047 (13.08266)	84.0334 (24.26707)	54.2231 (10.24193)
3.	18	17.1944 (6.58289)	191.7404 (11.66492)	22.1064 (5.75524)
4.	152	29.0090 (11.85610)	111.6571 (23.37250)	87.2211 (14.29215)
5.	75	21.7477 (7.55783)	147.5674 (30.22235)	60.3806 (15.65421)
6.	133	40.1941 (9.70592)	129.7167 (19.19727)	42.0610 (18.11304)
7.	102	15.9222 (9.16507)	57.2671 (19.88777)	19.6501 (11.18058)
8.	165	28.2070 (6.77547)	97.3685 (22.51146)	28.3771 (7.87864)
9.	5	13.3830 (8.02090)	118.3113 (18.78018)	134.9330 (6.90278)
10.	19	6.5834 (2.87575)	207.6139 (24.26852)	18.7894 (6.21197)
11.	32	23.5779 (8.93460)	71.6422 (13.32687)	44.5285 (9.93240)
12.	15	23.9388 (7.06852)	154.4370 (16.74696)	111.4998 (12.05213)

Table 5-5 (continued)

	No. of Pixels	4 1st Neighbor Contrast of Band 5	5 Tone of Band 7	6 1st Neighbor Contrast of Band 7
13.	398	12.0644 (6.76178)	130.1483 (16.74242)	12.0395 (6.29061)
14.	25	37.3664 (6.65471)	156.6532 (17.22484)	71.9099 (4.81088)
15.	26	41.3109 (7.09711)	167.2048 (18.20746)	34.5287 (10.00848)
16.	16	11.4480 (4.47998)	170.3331 (12.11936)	81.4426 (17.35971)
17.	19	16.9648 (8.90710)	121.3331 (21.22462)	24.8551 (7.09146)
18.	13	11.3974 (6.74258)	219.4356 (13.37675)	13.8333 (6.12970)
19.	18	9.7176 (4.97375)	80.7468 (16.46539)	74.9304 (14.91539)
20.	13	44.6602 (7.06248)	153.5125 (17.91463)	28.3076 (9.31876)
21.	5	10.8000 (5.07405)	177.9998 (19.78577)	50.3500 (3.20404)
22.	1	13.1670 (0.0)	193.7780 (0.0)	125.7500 (0.0)
23.	10	6.7001 (1.93075)	33.2778 (12.81612)	15.9584 (3.76965)
24.	1	6.3330 (0.0)	199.5560 (0.0)	87.3330 (0.0)
25.	2	18.8335 (0.16683)	129.4999 (11.72321)	114.1250 (3.62500)
26.	5	20.3168 (0.82754)	85.2001 (14.51710)	11.9500 (5.10980)
27.	3	15.8890 (6.90073)	190.2962 (13.78688)	60.1947 (4.98048)
28.	15	45.3110 (3.83847)	163.3777 (17.06926)	28.3999 (6.39148)
29.	6	10.9307 (4.54688)	119.0739 (12.86134)	129.7775 (9.85362)
30.	2	64.5835 (3.33366)	130.1664 (11.94551)	112.6665 (3.33424)
31.	4	57.4167 (14.67910)	151.9163 (12.55223)	27.1875 (3.36050)
32.	1	96.3330 (0.0)	150.8890 (0.0)	62.1670 (0.0)
33.	3	11.7223 (4.28506)	104.7036 (10.25533)	49.3056 (4.14560)
34.	1	64.2500 (0.0)	173.3330 (0.0)	40.2500 (0.0)
35.	4	9.7082 (5.81020)	157.0276 (8.52249)	58.4165 (5.46708)
36.	2	40.8330 (1.99994)	152.8329 (6.39122)	76.2500 (8.50000)
37.	2	10.8335 (0.58355)	96.8885 (17.55537)	51.9585 (4.45858)
38.	1	73.4170 (0.0)	174.0000 (0.0)	20.5000 (0.0)
39.	2	70.7500 (9.08295)	166.3329 (13.00120)	28.0000 (2.99996)
40.	1	94.1670 (0.0)	186.0000 (0.0)	15.0000 (0.0)
41.	2	112.1250 (8.37500)	206.6664 (6.33505)	

TABLE 5-6. Hit-rate Analysis of the Training Sets

Step 1 variables: B4 MEAN B4 CON 1 B5 MEAN B5 CON 1 B7 MEAN B7 CON 1

Rank of each set: C1 = 6 C2 = 6 C3 = 6 C4 = 6 C5 = 6 C6 = 6 C7 = 6 C8 = 6 C10 = 6
C11 = 6 C13 = 6 C23 = 6 C18 = 6

CONFUSION MATRIX

	C1	C2	C3	C4	C5	C6	C7	C8	C10	C11	C13	C19	C23	C18
C1	551	2	0	0	0	1	34	45	0	0	87	0	0	0
C2	0	61	0	5	0	6	3	1	0	1	1	0	0	0
C3	0	0	16	0	2	0	0	0	0	0	0	0	0	0
C4	0	2	0	132	6	3	7	0	0	1	0	1	0	0
C5	0	0	0	9	63	1	1	0	0	0	0	1	0	0
C6	0	10	0	3	3	108	1	7	0	0	1	0	0	0
C7	2	4	0	0	0	0	89	6	0	0	1	0	0	0
C8	7	6	0	0	0	18	11	120	0	2	1	0	0	0
C10	0	0	0	0	0	0	0	0	18	0	0	0	0	1
C11	0	0	0	0	1	0	9	0	0	22	0	0	0	0
C13	56	0	0	0	0	6	0	12	0	0	324	0	0	0
C19	0	0	0	0	0	0	0	0	0	0	0	18	0	0
C23	0	0	0	0	0	0	0	0	0	0	0	0	10	0
C18	0	0	0	0	0	0	0	0	1	0	0	0	0	12

Total Correct Classification = 79.88 percent.

SECTION 6

THE DIRECT METHOD

6.1 INTRODUCTION

This section describes an investigation of the direct method for modeling the texture variables as multivariate stable distributions. This modeling technique contrasts with the procedures described in Section 3 where a hybrid combination of normal distribution theory and stable distribution theory model is described. This hybrid model basically involves a coordinate-wise transformation of the texture variables so that each of the texture variables is by itself more nearly normal. After this transformation, the usual Mahalanobis classifier is used to carry out the discriminant analysis. The overall procedure has been called the stable Mahalanobis classifier. Based on the results of this study presented in Section 4, the stable Mahalanobis classifier considerably improves the number of correctly classified cases.

The potential difficulty with this method is that it does not properly account for the interaction among the texture variables. Specifically, intervariable correlations are changed after the transformations are applied. This means that a combination of two different texture variables which might give good classification before the normalizing classification, might give poor classification after the normalizing classification. In order to alleviate this difficulty, a direct method was studied. In this method, the texture variables are modeled directly as a multivariate stable distribution. The resulting models are quite complex and require a large volume of computation.

This section describes the direct method model as well as related computational procedures. We first begin by describing in Section 6.2 the characteristics of multivariate stable distributions in general. After this, we describe in Section 6.3 a restricted class of stable distributions which share important properties of the multivariate normal distribution. It is this class which we propose to model texture variables for a pixel by pixel classification of image data. After a description of this restricted model, we discuss estimation of parameters for this model in Section 6.4. This is followed by a discussion of classification procedures and discussion of the probability of correct classification in Section 6.5. Computational procedures are discussed in Section 6.6. Section 6.7 gives some general discussion of the method.

6.2 CHARACTERISTICS OF MULTIVARIATE STABLE DISTRIBUTIONS

Stable distributions and their potential have been known for a considerable length of time. The mathematical groundwork was laid by Paul Levy in 1925. Since then, a considerable development has occurred, but this development is still small compared to other areas of statistical modeling. One of the reasons for this slow development is that they do not have closed form expressions, except for special cases. Bergstrom (1952) obtained some series expansions for univariate stable densities. Until the availability of modern cheap computer power, work with these expansions has been difficult.

An important property of stable distributions is that the sum of two independent stable variates with the same characteristic α is itself stable with characteristic α. Another important property of stable distributions is that only stable distributions may be a domain of attraction. The importance of the normal distribution is due largely to the central limit theorem. When the random variables under consideration do not possess variances, limit theorems may still hold provided suitable norming constants are used. For this situation, the only possible limit distributions are stable distributions.

Stable distributions are useful in data analysis for modeling skewed data and heavy tailed distributions. Mandelbrot (1963-1967) has given a number of applications in the field of economics. More recently, Stuck and Kleiner (1974) have successfully modeled noise with stable distributions. Other examples of applications of stable distributions may be found in Press (1972) and Feller (1966).

As in the case of univariate stable distributions which are adequately described in Section 3, the theory of multivariate stable distributions is similar to the theory of multivariate normal distributions and in fact contains the normal theory as a special case. As in the univariate case, the multivariate stable distribution is best described by its characteristic function. We suppose that there are p random variables $Y_1, \ldots, Y_p$ which will generally be denoted by the random vector $Y = (Y_1, \ldots, Y_p)$. These variables correspond to the texture variables identified during earlier phases of this study.

The multivariate characteristic function depends on p variables $t_1, \ldots, t_p$ which are more conveniently expressed in vector form $t = (t_1, \ldots, t_p)$. Various representations of the characteristic function $\phi(t)$ are obtainable. The most useful form was obtained by Press (1972) and is given as

$$\log \phi(t) = ia't - \frac{1}{2}\sum_{j=1}^{m} (t'\Omega_j t)^{\alpha/2}(1 - i\beta(t) \tan \frac{\pi\alpha}{2})$$

for $\alpha \neq 1$. In this formula, $a = (a_1, \ldots, a_p)$ is the vector of location parameters; Ω_j is a p x p non-negative definite matrix of rank less than or equal to p; $\beta(t)$ is the skewness parameter and as in the univariate case the index is α where $0 < \alpha \leq 2$. If $\alpha = 2$, the distribution becomes the multivariate normal distribution with mean vector a and covariance matrix

$$\Sigma = \Omega_1 + \Omega_2 + \ldots + \Omega_p.$$

When $\beta(t) \equiv 0$, the distribution becomes symmetric. Most of the currently available literature and applications deal with symmetric stable distributions.

The properties of univariate stable distribution which make them attractive for data analysis carry over to multivariate stable distributions. In particular, the sum of two random vectors with multivariate stable distribution of the same index , also has a multivariate stable distribution of index α. Multivariate stable distributions also possess domains of attraction.

One of the important properties of multivariate normal distributions is that every linear combination of its components has a univariate normal distribution. This property can be used to characterize the multivariate normal distribution. The property also carries over to stable distributions. That is, every linear combination of the components of a multivariate stable distribution has a univariate stable distribution. The characteristic α of the resulting univariate stable distribution is the same as that of the multivariate stable distribution. Moreover, if the multivariate stable distribution is symmetric, so will the univariate be symmetric.

Unlike normal distributions, stable distributions can be used to model skewed and heavy tailed data.

6.3 A RESTRICTED MODEL

There are various possible types of multivariate stable densities. The general model developed by Press (1972) and described in Section 6.2 is too general for purposes. Depending on the structure of the matrices Ω_j and the number of terms in the sum forming the characteristic function, certain models do not allow for independence of the coordinate variables.

As part of this study, we have re-examined the most general form of the characteristic function for multivariate stable distribution as it was developed by Paul Levy in 1925. We developed a form similar to that of Press, but more suitable for our purposes. We describe this development in more detail later. This different form permits us to obtain probability density functions for a certain restricted class of multivariate stable distributions. These densities have properties analagons to the multivariate normal distributions. In particular, they admit of a decomposition similar to the principle components decomposition for normal distributions.

This decomposition permits one to evaluate the multivariate stable density function by evaluating a series of univariate stable density functions. This feature of our restricted model greatly reduces the amount of computation required in evaluating the multivariate stable density function which will be needed by the maximum likelihood classifier algorithm. An additional feature of this decomposition is that it permits the study of multiple colinearities which exist among the texture variables. This problem was identified while working with the normal distribution model and solved by using the generalized inverse of the singular within target class covariance matrices. It also provides a method of using a step wise procedure on linear combinations of texture variables similar to that used in factor analysis under normal distribution models.

Our starting point is a representation of the characteristic function for multivariate stable distributions which was obtained by Levy in 1925 using the fact that stable distributions are infinitely divisible and other properties of stable distributions. This representation of the log characteristic function is

$$\log \phi(t) = i\,P_1(t) - \frac{1}{2}P_2(t) + \int_{B}\int_{0}^{\infty}\left\{e^{irt'w} - 1 - \frac{irt'w}{1+r^2}\right\}\frac{dr}{r^{\alpha+1}}\,d\phi(w)$$

where $|w| = (w'w)^{\frac{1}{2}} = 1$; i.e., w ranges over the n dimensional unit sphere B and is weighted according to a finite measure $\phi(w)$ over the surface of the n dimensional unit sphere. The integration is essentially in spherical coordinates over the n dimensional sphere.

After suitable developing this integration, we obtained a slightly different, but more useful form of the characteristic function which permitted us to define a restricted class of stable densities with the properties described at the beginning of this section.

6.4 ESTIMATION OF PARAMETERS

Press (1972) discusses some methods for estimation of parameters for multivariate stable distributions. Most of his discussion centers on a special class of symmetric multivariate stable distributions whose characteristic function is given by

$$\log \phi(t) = ia't - \frac{1}{2}(t'\Omega t)^{\alpha/2}.$$

His methods are not useful to the purposes of this study. His model is quite different from ours and his methods and model seem inapplicable. General methods for estimation of parameters in general multivariate stable distributions seem to be unavailable in the literature. However, for our restricted model, the density is reducible to a sequence of univariate densities preceded by a suitable matrix transformation.

Therefore, we use the methodology developed for the univariate estimation problem. These procedures are described in Section 3 of this report. There are two options open. The first is the maximum likelihood method and the other is the fast method. An overall maximum likelihood model has been developed for our restricted model. We can also use a two stage iterative procedure consisting of a rotation estimate followed by a series of univariate maximum likelihood estimates. This offers an attractive alternative in terms of processing time.

6.5 CLASSIFICATION PROCEDURES

Our classification procedures consist of a maximum likelihood discriminant analysis adapted to stable distributions. The objective here is to use the texture variables identified as important for classification during the training phase of our procedure. Different texture variables are permitted for each class: soil, vegetation, etc.

It is assumed that the texture variables of the objects have density functions $P_1(Y)$, ..., $P_k(Y)$ where $P_i(Y)$ is the density function for the objects in the i th class. The standard method for classification of an unknown object whose vector of texture variables is given as Y is to compute the numerical value of $P_i(Y)$ for each i = 1,..., k and place the object into class i_o for which $P_{i_o}(Y)$ is largest. This method is described for example in Rao (1973) (p. 574). In case the $P_{i_o}(Y)$'s are multivariate normal, this method leads to the usual linear discriminant function. The method can also be modified to incorporate a prior distribution π_i, i = 1, ..., k if a Bayesian approach is desired. In this case, the quantities $\pi_i P_i(Y)$ are computed for i = 1, ..., k and the object whose vector of texture variables is Y is placed in the class which maximizes $\pi_i P_i(Y)$ for i = 1, ..., k. For our work, we omitted the Bayesian approach. It is referred to here for completeness of the theory only.

The decision procedure described here allows for a variety of shapes to the decision boundaries. This is in contrast to the normal theory where the constant probability curves for each of the training classes assumed normally distributed is elliptical.

The classification procedure can be summarized as follows: Step One is the training phase during which the maximum likelihood procedure is used to estimate parameter values for the principal components of the univariate stable distributions. Also during the training phase the parameters of the linear transformation are determined. A subset of the texture values is shown for each of the training classes which is found to be most useful for classification purposes. Step Two of the classification procedure consists of a pixel by pixel transformation of the relevant texture variables for each class and then an evaluation of the univariate stable density functions corresponding to each of the principal components used for that class. The pixel is then classified into the class for which the density is maximum.

6.6 PROBABILITY THAT A PIXEL BELONGS TO A CLASS

The classification procedure described in Section 6.5 forces each pixel to be classifed into one of the alternative classes even if it does not readily fit into that class. This situation also arises in classification procedures using normal distribution theory. As in the case of normal models, the direct method for the restricted class of stable models we considered can yield the probability that a given pixel will deviate from the class centroid by as much as the observed deviation. This probability is calculated in the same way that the classification is calculated. First a linear transformation is applied to the texture variables to obtain the values of the principal components. A univariate probability is calculated for each of the principal components. These components are independent. This permits us to form their product to obtain the overall probability that the given pixel deviates from the class centroid by the observed amount.

This procedure permits us to have unclassified pixels in the decision map, if they do not fit reasonably well into the class which the maximum likelihood procedure assigns them. This entire procedure is completely analogous to the one we used for the normal distribution case.

6.7 ADVANTAGES OF THE DIRECT METHOD

The direct method proceeds in the following way. For each training class, a maximum likelihood estimate of the linear transformation which produces principle components of the texture variables along with a maximum likelihood estimates of the stable distribution parameteters of these components is obtained. The maximum likelihood procedure is an iterative computational procedure. Confusion matrices are obtained in the usual way of classifying each of the pixels in the training set and counting the number of correctly classified pixels. Classification of unknown pixels consists of transforming the texture variables of the unknown pixels to the corresponding principle components followed by an evaluation of a series of univariate stable density functions and then a classification of the pixel into the group it most likely belongs. At the option of the operator, a pixel can be left unclassified if it does not belong to any group with a reasonable probability level.

The main advantage of the direct method is that it utilizes the intervariable correlation structure which exists among the texture variables. The indirect method, on the other hand, alters this structure. At the same time all of the advantages of the normal method are retained. One can obtain the probability that a point belongs to none of the training classes. This permits one to obtain undecided categories. The overall model approach to fitting parameters should give better results than the indirect method. An overall evaluation of this point is not available at this time because the method is not yet implemented.

REFERENCES CITED

1. Bergstrom, H., "On Some Expansions of Stable Distribution Functions," Arkiv for Mathematik, 2:375-378 (1952).

2. Crane, R.B., Malina, W.A., and Richardson, W., "Suitability of the Normal Density Assumption for Processing Multi-spectral Scanner Data," IEEE Transaction on Geoscience Electronics, Vol. GE10 (1972) pp. 158-167.

3. DuMouchel, W.H., Stable Distributions in Statistical Inference. Ph.D. Dissertation, Yale University, 1971.

4. Fama, E.F., and Roll, R., "Some Properties of Symmetric Stable Distributions," Journal of the American Statistical Associations, Vol. 63 (1968), pp. 817-836.

5. ______(Unknown)______, "Parameter Estimates for Symmetric Stable Distributions," Journal of the American Statistical Association, Vol. 66 (1971), pp. 331-338.

6. Feller, W., An Introduction to Probability and Its Applications, Vol. II, New York, Wiley (1966).

7. Foley, D., "The Probability of Error in the Design Set as a Function of the Sample Size and Dimensionality," Technical Report RADC-TR-71-171, 1971. AD# 738 648.

8. Glick, N., "Additive Estimators for Probabilities of Correct Classification," IEEE, Pattern Recognition and Image Processing (1977), pp. 304-317.

9. Hsu, S., and E. Klimko, Texture Feature Extraction and Analysis, Rome Air Development Center, 1977. (RADC-TR-77-279, Final Technical Report.) AD# A045 542

10. Julesz, B., "Experiments in the Visual Perception of Texture," Scientific America (1974), pp. 34-43.

11. Levy, P., Calcul des Probabilities (1925), Ganthier-Villars, Paris.

12. Mandelbrot, B., "The Stable Paretian Income Distribution When the Apparent Exponent is Near Two," International Economic Review 4 (1963a), pp. 111-114.

13. Mandelbrot, B., and Taylor, H.M., "On the Distribution of Stock Price Differences," Operations Research (1967) 15: 1057-1062.

References Cited (continued)

14. Masters, T., "Estimation of Parameters for Univariate Stable Distributions," Masters Thesis, State University of New York at Binghamton, 1977.

15. Morrison, D.F., Multivariate Statistical Methods, New York: McGraw-Hill (2nd edition), 1976.

16. Nalepka, R., "Investigation of Multispectral Discrimination Techniques," Report No. 2264-12-F Willow Run Laboratories, Institute of Science and Technologies, University of Michigan, 1970.

17. PAR/RADC Digital Image Processing Techniques for Automatic Terrain Classification for Generating Reference Maps for B/W Aerial Photography, RADC, 1976.

18. Paulson, A.S., Holcomb, E.W., and Leitch, R.A., "The Estimation of the Parameters of the Stable Laws," Biometrika, 62 (1975), pp. 163-168.

19. Press, S.J., "Multivariate Stable Distributions," Journal of Multivariate Analysis, Vol. 2, 1972, pp. 444-462.

20. (Unknown) , "Estimation in Univariate and Multivariate Stable Distributions," Journal of the American Statistical Association, Vol. 67, 1972(a), pp. 842-846.

21. (Unknown) , Applied Multivariate Analysis. New York, Holt Rienhart and Winston, Inc., 1972(b).

22. Rao, C.R., Linear Statistical Inference and Applications (2nd edition). New York, Wiley, 1973.

23. Rao, C.R. and Mitra, S.K., Generalized Inverse of Matrices and Its Applications, New York: Wiley, 1971.

24. Rome Air Development Center, Griffiss Air Force Base, Rome, New York, Statement of Work for Automatic Feature Extraction System (AFES), 1976.

25. Searle, S.R., Linear Models, Wiley, New York, 1971.

26. Stuck, B.W., Kleiner, B., "A Statistical Analysis of Telephone Noise," Bell System Technical Journal 53, No. 7, pp. 1263-1312 (1974).

MISSION
of
Rome Air Development Center

RADC plans and executes research, development, test and selected acquisition programs in support of Command, Control Communications and Intelligence (C^3I) activities. Technical and engineering support within areas of technical competence is provided to ESD Program Offices (POs) and other ESD elements. The principal technical mission areas are communications, electromagnetic guidance and control, surveillance of ground and aerospace objects, intelligence data collection and handling, information system technology, ionospheric propagation, solid state sciences, microwave physics and electronic reliability, maintainability and compatibility.